Materials Science-Poland, 33(1), 2015, pp. 100-106
http://www.materialsscience.pwr.wroc.pl/
DOI: 10.1515/msp-2015-0027

DE GRUYTER OPEN

Influence of different synthesis conditions on properties of oleic acid-coated-Fe_3O_4 nanoparticles

ATIEH ALIAKBARI, MAJID SEIFI*, SHARAREH MIRZAEE, HODA HEKMATARA

Department of Physics, Faculty of Science, University of Guilan, Rasht, 41335-1914, Iran

In the present paper, iron oxide nanoparticles coated by oleic acid have been synthesized in different conditions by co-precipitation method. For investigating the effect of time spent on adding the oleic acid to the precursor solution, two different processes have been considered. The as synthesized samples were characterized by X-ray diffraction (XRD), transmission electron microscopy (TEM) and Fourier transform infrared spectroscopy (FT-IR). Magnetic measurement was carried out at room temperature using a vibrating sample magnetometer (VSM). The results show that the magnetic nanoparticles decorated with oleic acid decreased the saturation of magnetization. From the data, it can also be concluded that the magnetization of Fe_3O_4/oleic acid nanoparticles depends on synthesis conditions.

Keywords: *co-precipitation; super-paramagnetic nanoparticles; oleic acid; strain; magnetite*

1. Introduction

Ferrites with the general formula AB_2O_4 have attracted much attention due to their wide applications, such as data storage [1], magnetic resonance imaging (MRI) contrast agents [2], magnetically guided drug delivery [3], and catalysis [4]. Among the ferrites, magnetite is a frequently used magnetic nanoparticle (MNP) because of its high saturation magnetization, ease for bio-molecule tagging, and bio-compatibility [5, 6]. The magnetite (Fe_3O_4) has an inverse spinel structure, which contains iron cations in mixed oxidation states with $Fe^{3+}(Fe^{2+}Fe^{3+})O_4$ formula. In this structure, the oxygen atoms form a face-centered cubic close-packed array and the half of the ions are tetrahedrally coordinated, while the other half of the Fe^{3+} ions and all of the Fe^{2+} ions are octahedrally coordinated [7].

The aforementioned ferrite has unique electrical and magnetic properties based on the transfer of the electrons between the Fe^{2+} and Fe^{3+} ions in the octahedral sites. However, MNPs show novel properties, which are different from those of the bulk materials, due to their small size and fundamental changes in the coordination, symmetry and confinement [8]. One of the most common methods for synthesizing the iron oxides in nanoscale regime is the chemical co-precipitation due to low cost and easy synthesis process [9], however, in this method it seems to be a large tendency to agglomeration and MNPs are susceptible to air oxidation [10, 11].

According to the previous works, modification of the surface of Fe_3O_4 nanoparticles during the synthesis by organic materials, like polymers [12–16] and fatty acid [17–25], can reduce the aggregation and prevent the possible air oxidation. Most of the aforementioned studies, which concerned the oleic acid, have been focused on the variations of parameters, like temperature, pH, amount of surfactant and stirring speed.

To the best knowledge of the authors, the effect of time, in which the oleic acid adds to the mixture, has not been studied so far. Hence, in this paper, we synthesized pure and oleic-acid-coated Fe_3O_4 particles in two different conditions by co-precipitation method. The results show that the process of addition of oleic acid to the precursors can affect the structure and size of the spinel ferrite and change the magnetic properties of MNPs.

*E-mail: m_seifi2000@yahoo.com

2. Experiments

2.1. Materials

All chemical materials, including iron chloride hexahydrate $FeCl_3 \cdot 6H_2O$, iron sulfate heptahydrate $FeSO_4 \cdot 7H_2O$ and oleic acid ($C_{17}H_{33}COOH$), which were purchased from the Merck Chemical Corporation, were used as received without further purification.

2.2. Synthesis of pure Fe_3O_4 NPs

The flowchart of magnetite nanoparticles preparation is shown in Fig. 1. At first, 2.59 g of ferrous chloride hexahydrate and 1.33 g of ferric sulfate heptahydrate were dissolved into 100 mL of distilled water, separately. Then these two solutions were mixed together under the Ar atmosphere at 80 °C. In the next step, ammonia solution (25 mL) as a precipitant was added dropwise to the reaction solution under the vigorous magnetic stirring and Ar atmosphere for 30 minutes. The black precipitate was washed several times with distilled water. Finally, the product was dried in an oven at 70 °C for 12 hours. The sample from uncoated Fe_3O_4 nanoparticles was labeled as sample a.

2.3. Surface coating with the oleic acid

Sample b: 5 mL of oleic acid was dissolved in 5 mL of acetone and then, the oleic acid solution was mixed with the solution of precursors all at once at room temperature and under the Ar atmosphere, before adding ammonia solution. After that, 25 mL of ammonia solution was added dropwise to the mixture at 80 °C and stirred for one hour. Sample c: at first ammonia solution was added dropwise to the solution of precursors at 80 °C under the Ar atmosphere for 30 min. Then, the oleic acid solution was added dropwise to the mixture for one hour. In both samples the black precipitate was washed several times with n-hexan and distilled water to remove the remaining oleic acid and impurities, then the samples were dried at 70 °C for 12 hours.

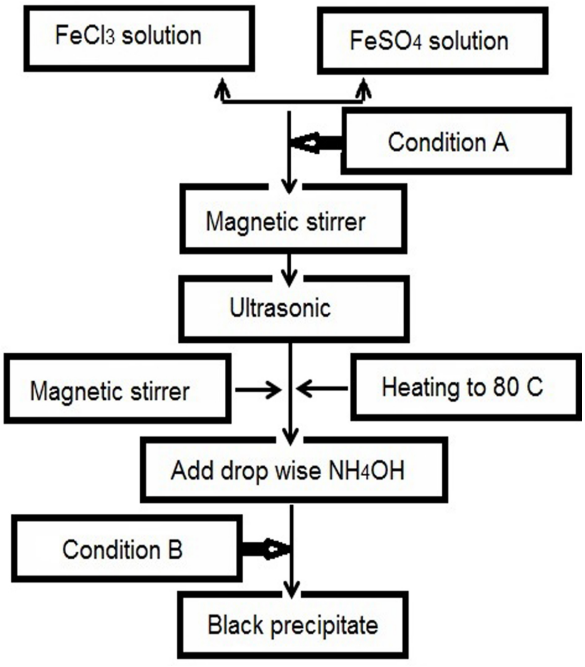

Fig. 1. Flow chart of magnetite nanoparticles preparation.

2.4. Characterization

The as synthesized samples were characterized by X-ray diffractometer (XRD) using a PW 1800 (Philips, Netherland) and CuKα radiation ($\lambda = 0.154$ nm). In order to calculate crystallite size, the Scherrer's formula was applied. For evaluation of the interaction between oleic acid and Fe_3O_4 nanoparticles (FT-IR) spectra of KBr pellets were measured with the Fourier transform infrared spectrometer (Nicolet Magna, IR 560, USA) in transmission mode. Magnetization of the specimens was measured by vibrating sample magnetometer (VSM), (Meghnatis Daghigh Kavir Co., Iran). The morphology of nanoparticles was observed by transmission electron microscopy (Philips CM 10).

3. Results and discussion

3.1. XRD

The XRD patterns of the samples are shown in Fig. 2. As can be seen, all the samples have the cubic spinel structure and pure phase of Fe_3O_4 is confirmed by the diffraction peaks, which are well matched with the standard diffraction

spectrum (JCPDS Card No.19-0629), [26–28]. Also the black color of the products further testifies that they contain solely the magnetite phase, not the maghemite phase. It has also been shown in section 3.4 that our samples have a high saturation magnetization of about 62 emu/g. It is worth mentioning that the magnetite has a higher magnetization value than that of the maghemite (of 30 to 40 emu/g [29, 30]). Consequently, the as synthesized samples have the saturation magnetization corresponding to magnetite.

In addition, the XRD patterns show that the presence of oleic acid in the synthesis has not changed the structure of obtained magnetite nanoparticles.

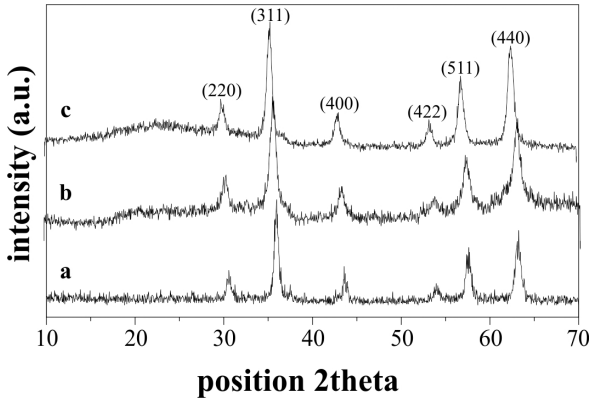

Fig. 2. X-ray diffraction patterns of iron oxide nanoparticles corresponding to samples a, b and c.

The two main properties obtained from the peak width analysis are crystallite size and lattice strain. The average crystallite size corresponding to the (311) diffraction peak of the strongest intensity was calculated by the Scherrer's formula [31]:

$$D = \frac{K\lambda}{\beta \cos\theta} \tag{1}$$

where D is the average crystallite size of nanoparticles, λ is the wavelength of incident X-ray (0.154 nm), K is the shape factor (0.9), β denotes the full width at half-maximum, and θ is the angle of the strongest peak. The results show that the crystallite size of samples a, b and c is about 18, 9 and 11 nm, respectively.

The crystallite size and lattice strain of the samples have been also estimated using the Williamson-Hall (W-H) equation [32]:

$$\beta \cos\theta = \frac{k\lambda}{D} + 4\varepsilon \sin\theta \tag{2}$$

where ε is the strain distribution within the nanoparticles. Equation 2 represents the uniform deformation model (UDM), where the strain was assumed to be uniform in all crystallographic direction. The crystallite size was estimated from the y-intercept and the strain ε obtained from the slope of the fit.

The W-H plots of all the samples (using the best linear fit to data) are shown in Figs 3, 4 and 5. The results of W-H calculations show that the crystallite sizes of the samples a, b, c are 20, 11 and 13 nm, respectively. In addition, the obtained amounts of strain are 0.0011, 0.0005 and 0.0004.

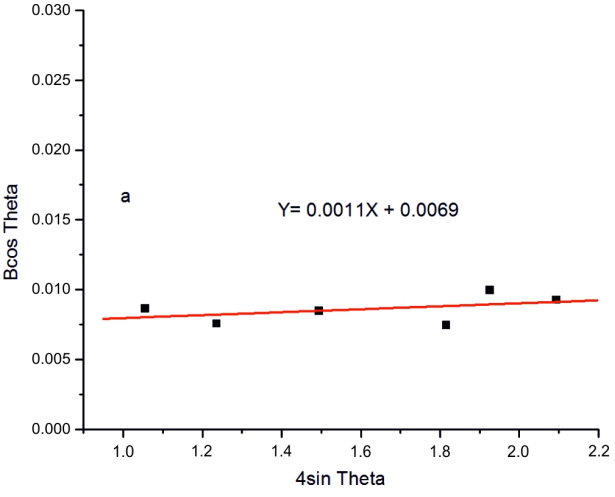

Fig. 3. The plot obtained from the W-H analysis of the sample a.

3.2. TEM

Morphology and mean particle size of prepared pure magnetite nanoparticles were determined by TEM (Fig. 6). The particles are quasi-spherical and have the size ranging from 18 to 22 nm. Also, the particle size was estimated from TEM, which was consistent with XRD result.

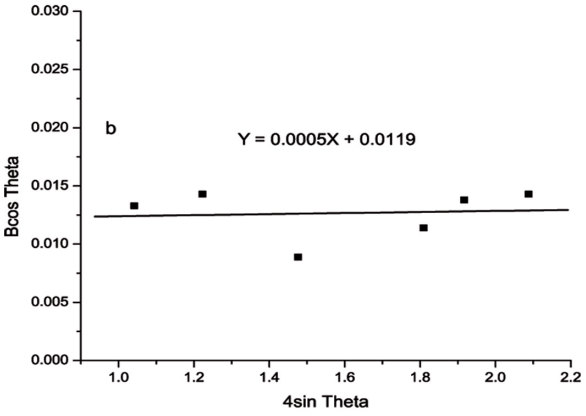

Fig. 4. The plot obtained from the W-H analysis of the sample b.

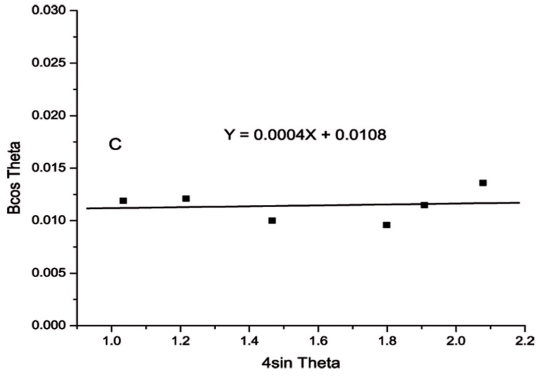

Fig. 5. The plot obtained from the W-H analysis of the sample c.

3.3. FT-IR

To investigate the formation of the interaction between Fe_3O_4 nanoparticle and its oleic acid shell, FT-IR spectroscopy has been used. Fig. 7d shows the FT-IR spectra of a pure oleic acid. The dips at 2926 and 2858 cm^{-1} are due to the symmetric and asymmetric stretching vibration of CH_2 [33]. An absorption band at 1711 cm^{-1} presents the stretching vibration of carboxyl group (C=O). The O–H in-plane and out-of-plane bands appear at 1455 and 939 cm^{-1}, respectively. The characteristic absorption band at 1286 cm^{-1} corresponds to the bending vibration of C–O.

In the case of uncoated iron oxide nanoparticles, the bond at 3386 cm^{-1} is assigned to stretching (ν) vibrations and the band at 1625 cm^{-1} is assigned to bending (δ) vibrations due to adsorbed water on the surface of iron oxide nanoparticles [34]. The two distinct absorption peaks at 447 and 570 cm^{-1} are attributed to the stretching vibration of Fe–O bonds in the octahedral and tetrahedral sites [35].

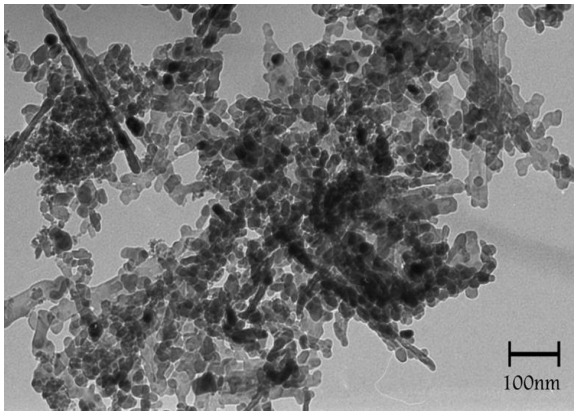

Fig. 6. TEM image of the sample a.

Table 1. The average crystallite size and strain of the pure and coated MNPs.

Strain	**Williamson-Hall method** (nm)	**Debye-Scherrer method** (nm)	**Sample**
0.0011	20	18	a
0.0005	11	9	b
0.0004	13	11	c

Fig. 7b and 7c show the FT-IR spectra of the Fe_3O_4 /oleic acid samples. Comparing with the spectrum of pure oleic acid (Fig. 7d), in the samples b and c, the C–H asymmetric bending vibration shifted to 2922 and 2920 cm^{-1} and the C–H symmetric bending vibration shifted to 2853 and 2852 cm^{-1}, respectively.

As a result, the characteristic bands shifted to a lower frequency region, which indicates the hydrocarbon chains in the monolayer surrounding the nanoparticles in a close-packed crystalline state [36].

The sharp dip at 1711 cm^{-1} disappeared in the spectra of the coated nanoparticles (Fig. 7, samples a and c), and two new dips are observed at 1532, 1639 cm^{-1} (sample b) and 1562, 1627 cm^{-1} (sample c), which correspond to the asymmetric

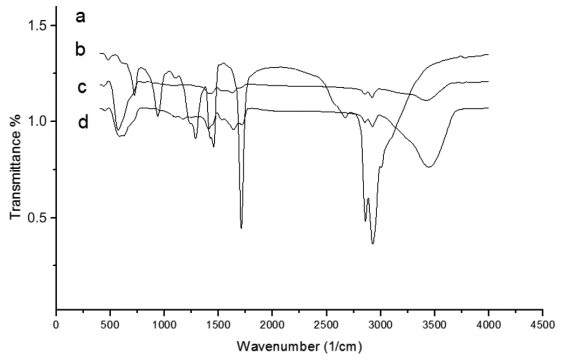

Fig. 7. The FT-IR spectra of the samples a – c and pure oleic acid d.

and symmetric stretching vibrations of (COO^-), respectively [37, 38]. This can be explained in such way that the carboxyl groups of oleic acid combined with the Fe atoms on the surface of Fe_3O_4 nanoparticles.

The characteristic IR bands of oleic acid and other samples have been summarized in detail in Table 2.

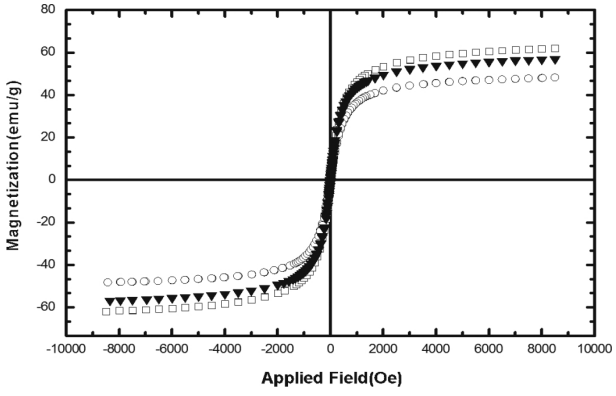

Fig. 8. The hysteresis loops of samples a – c.

3.4. VSM

The magnetic properties of Fe_3O_4 and oleic acid coated Fe_3O_4 nanoparticles were investigated using a vibrating sample magnetometer (VSM) at room temperature. Fig. 8 shows the magnetization as a function of the applied magnetic field between −10 and 10 KOe. There is no pronounced hysteresis loop, which indicates that both retentivity and coercivity of the composites are zero. This observation is consistent with the superparamagnetic behavior of all samples [39–41].

Table 2. Assignment of FT-IR spectra of uncoated iron oxide, oleic acid coated iron oxide, and pure oleic acid.

Description	**IR region or band** (1/cm)	**Samples**
Uncoated iron oxide a	447	ν (Fe–O)
	570	ν (Fe–O)
	1625	δ (H–O)
	3386	ν (H–O)
Oleic acid coated iron oxide b	451	ν(Fe–O)
	589	ν (Fe–O)
	1407	δ (C–H)
	1532	ν_{as} (COO)
	1639	ν_s (COO)
	2853	ν_s (C–H)
	2922	ν_{as} (C–H)
	3445	ν (H–O)
Oleic acid coated iron oxid c	439	ν (Fe–O)
	574	ν (Fe–O)
	1419	δ (H–O)
	1562	ν_{as} (COO)
	1627	ν_s (COO)
	2852	ν_s (C–H)
	2920	ν_{as} (C–H)
	3423	ν (H–O)
Pure oleic acid d	939	O–H out-of-plane
	1288	
	1455	ν (C–O)
	1711	O–H in-plane
	2858	ν (C=O)
	2926	ν_s (C–H)
		ν_{as} (C–H)

The obtained value of the saturation magnetization for the pure magnetite nanoparticles is about 62 emu/g, which is obviously smaller than that of its bulk value. That can be attributed to the smaller particle sizes. The more the decrease in particle size, the larger the surface spin canting, and, consequently, a significant reduction in the magnetization value is obtained [42]. Therefore, the smaller particles apparently have lower magnetization. The saturation magnetization value of the samples b and c are about 48 and 57 emu/g, respectively. This lowering is due to the smaller size of the coated particles and the presence of a non-magnetic oleic

acid coating on the surface of the particles. In the sample b the oleic acid was added to the precursors all at once in comparison to the sample c, which caused defects in cubic lattice. Consequently, the nanoparticles experienced the strain. According to Table 1 the amount of strain in the sample b is higher than in the sample c. In addition, it is known that strains tend to reduce the saturated magnetization. Hence, the amount of saturation magnetization in sample b is lower than in the sample c.

4. Conclusions

We have shown that the modified co-precipitation method for synthesizing oleic acid coated Fe_3O_4 nanoparticles, carried out in two different processes, can affect the magnetic properties of MNPs, like the size and saturation magnetization. We revealed that the coated nanoparticles had a smaller size with respect to the pure nanoparticles. The dependence of magnetization on the size of the nanoparticles has been clearly shown in this paper. For smaller nanoparticle sizes, magnetization decreased. The amounts of strain in the as-synthesized samples were determined from the W-H method. The results showed that when the oleic acid was added to the solution of precursors all at once, the size of MNPs was smaller than in the case when the oleic acid was added to the mixture of the precursors dropwise, but the amount of strain in the samples obtained in the first process was higher than in the second one. All the aforementioned factors resulted in lowering the saturation magnetization in sample b.

References

[1] REISS G., HUTTEN A., *Nat. Mater.*, 4 (2005), 725.

[2] TAN H., XUE J.M., SHUTER B., LI X., WANG J., *Adv. Funct. Mater*, 20 (2010), 722.

[3] KIM J., LEE J.E., LEE S.H., YU J.H., LEE J.H., PARK T.G., HYEON T., *Adv. Mater*, 20 (2008), 478.

[4] WANG C., DAIMON H., SUN S., *Nano Lett.*, 9 (2009), 1493.

[5] SUN S., ZENG H., ROBINSON D.B., RAOUX S., RICE P.M., WANG S.X., LI G., *J. Am. Chem. Soc.*, 126 (2004), 273.

[6] ZHANG Y., KOHLER N., ZHANG M., *Biomaterials*, 23 (2002), 1553.

[7] O'HANDLEY R.C., *Modern Magnetic Materials: Principles and Applications*, John Wiley & Sons, New York, 2000.

[8] LESLIE-PELECKY D.L., RIEKE R.D., *Chem. Mater.*, 8 (1996), 1770.

[9] LAURENT S., FORGE D., PORT M., ROCH A., ROBIC C., ELS V.L., MULLER R., *Chem. Rev.*, 108 (2008), 2064.

[10] CORNELL R.M., SCHERTMANN U., *The Iron Oxides: Structure, Properties, Reactions, Occurrence and Uses*, VCH Publishers, Weinheim, Germany, 2003.

[11] HARRIS L.A., *Polymer stabilized magnetite nanoparticles*, Ph.D. Thesis, Virginia Polytechnic Institute and State University, Virginia, 2002.

[12] PARDOE H., CHUA-ANUSORN W., ST PIERRE T.G., DOBSON J., *J. Magn. Magn. Mater.*, 225 (2001), 41.

[13] GHOTBI M.Y., HUSSEIN M.B., *J. Phys. Chem. Solids*, 73 (2012), 936.

[14] CHOI S.H., ZHANG Y.P., GOPALAN A., LEE K.P., KANG H.D., *Colloid. Surface. A*, 256 (2005), 165.

[15] JIAN P., FEN Z., LU L., LIANG T., LI Y., WEI CH., HUI L., JING-BO T., LI-XIANG W., *T. Nonferr. Metal. Soc.*, 18 (2008), 393.

[16] KAYAL S., RAMANUJAN R.V., *Mat. Sci. Eng. C-Mater.*, 30 (2010), 484.

[17] TOMIKATA A., KOSHI T., HATSUGAI SH., YAMADA T., TAKEMURA Y., *J. Magn. Magn. Mater.*, 323 (2011), 1398.

[18] LI D., JIANG D., CHEN M., XIE J., WU Y., DANG SH., ZHANG J., *Mater. Lett.*, 64 (2010), 2462.

[19] GNANAPRAKASH G., MAHADEVAN S., JAYAKUMAR T., KALYANASUNDARAM P., PHILIPH J., RAJ B., *Mater. Chem. Phys.*, 103 (2007), 168.

[20] WANG CH. Y., HONG J. M., CHEN G., ZHANG Y., GU N., *Chinese Chem. Lett.*, 21 (2010), 179.

[21] LIN J., WANG CH., LEE M., *J. Magn. Magn. Mater.*, 332 (2013), 192.

[22] FENG J., MAO J., WEN X., TU M., *J. Alloy. Compd.*, 509 (2011), 9093.

[23] MAITY D., AGRAWAL D.C., *J. Magn. Magn. Mater.*, 308 (2007), 46.

[24] WEI Y., HAN B., HU X., LIN Y., WANG X., DENG X., *Procedia Eng.*, 27 (2012), 632.

[25] INGRAM D., KOTSMAR C., YOON K.Y., SHAO S., HUH CH., BRYANT S., MILNER TH., JOHNSTON K., *J. Colloid Interf. Sci.*, 351(2010), 225.

[26] VERIANSYAH B., KIM J.D., MIN B.K., KIM J., *Mater. Lett.*, 64 (2010), 2197.

[27] AHMAD M.A., OKASHA N., EL-DEK S.I., *Ceram. Int.*, 36 (2010), 1529.

[28] CABRERA L., GUTIERREZ S., MENENDEZ N., MORALES M.P., HERRASTI P., *Electrochim. Acta*, 53 (2008), 3436.

[29] ALIAHMAD M., NASIRI MOGHADDAM N., *Mater. Sci.-Poland*, 31 (2013), 264.

[30] CULLITY B.D., *Introduction to Magnetic Materials*, Addison-Wesley Publishing Company, Reading, Massachusetts, 1972.

[31] FAIYAS A.P.A., VINOD E.M., JOSEPH J., GANESAN R., PANDEY R.K., *J. Magn. Magn. Mater.*, 322 (2010), 400.

[32] KHORSAND ZAK A., ABD MAJID W.H., ABRISHAMI M.E., YOUSEFI R., *Solid State Sci.*, 13 (2011), 251.

[33] LEE S.Y., HARRIS M.T., *J. Coll. Interf. Sci.*, 293 (2006), 401.

[34] GIRI J., THAKURTA S.G., BELLARE J., NIGAM A.K., BAHADUR D., *J. Magn. Magn. Mater.*, 293 (2005), 62.

[35] AHN Y., CHOI E.J., KIM E.H., *Rev. Adv Mater. Sci*, 5 (2003), 477.

[36] NAKAMOTO K., *Infrared and Raman Spectra of Inorganic and Coordination Compounds*, Wiley, New York, 2009.

[37] REN Y., LIMURA K., KATO T., *Langmuir*, 17 (2001), 2688.

[38] WILLIS A.L., TURRO N.J., O'BRIEN S., *Chem. Mater.*, 17 (2005), 5970.

[39] MONTAGNE F., MONDAIN-MONVAL O., PICHOT C., MOZZANEGA H., ELAISSARI A., *J. Magn. Magn. Mater.*, 250 (2002), 302.

[40] MORALES M.P., ANDRES-VERGES M., VEINTEMILLAS-VERDAGUER S., MONTERO M.I., SERNA C.J., *J. Magn. Magn. Mater.*, 203 (1999), 146.

[41] SKOMSKI R., *Simple Models of Magnetism*, Oxford University, New York, 2008.

[42] RAJENDRAN M., PULLAR R.C., BHATTACHARYA A.K., DAS D., CHINTALAPUDI S.N., MAJUMDAR C.K., *J. Magn. Magn. Mater.*, 232 (2001), 71.

Received 2014-06-15
Accepted 2014-12-03